International Journal of Non-Linear Mechanics 126 (2020) 103560

Contents lists available at ScienceDirect

International Journal of Non-Linear Mechanics

journal homepage: www.elsevier.com/locate/nlm

Implicit constitutive relations for visco-elastic solids: Part II. Non-homogeneous deformations

R. Bustamante [a,*], K.R. Rajagopal [b], O. Orellana [c], R. Meneses [d]

[a] Departamento de Ingeniería Mecánica, Universidad de Chile, Beauchef 851, Santiago Centro, Santiago, Chile
[b] Department of Mechanical Engineering, University of Texas A&M, College Station, TX, USA
[c] Departamento de Matemáticas, Universidad Técnica Federico Santa María, Avenida España 1680, Valparaíso, Chile
[d] Escuela de Ingeniería Civil, Universidad de Valparaíso, General Cruz 222, Valparaíso, Chile

ABSTRACT

A constitutive relation was developed in Part I for describing the response of a class of visco-elastic bodies, wherein the left Cauchy–Green tensor, the symmetric part of the velocity gradient, and the Cauchy stress tensor are related through an implicit constitutive relation. Here, we study a boundary value problem within the context of the model namely the inhomogeneous deformation of the body, corresponding to the response of an infinitely long slab due to the influence of gravity.

1. Introduction

Illustrious scientists, the likes of Kelvin [1], Voigt [2] and Boltzmann [3] were amongst the early contributors to the development of constitutive relations for viscoelastic solids. A discussion of the early development, as well as the efforts of Rivlin, Green, Spencer, Pipkin, and others in the 1960s can be found in [4,5]. Recently, Rajagopal [6] introduced an implicit relationship between the history of the stress and the histories of the appropriate kinematical variables that includes as a special case generalizations of the Kelvin–Voigt constitutive relation, namely an implicit constitutive relation between the stress, the Cauchy–Green tensor and the symmetric part of the velocity gradient (see Rajagopal [7] and Bulicek et al. [8]). Much of the work concerning the response of viscoelastic solids is either restricted to small displacement gradients (linearized response, see Christensen [9], Wineman and Rajagopal [10]) or quasi-linear response with regard to biomaterials (see Fung [11]) and the recent generalization of quasi-linear response, see Muliana et al. [12]. Non-linear response focusing on the deformations of membranes have been put into place by Wineman [13–15] but even these simple problems lead to the numerical solution of complicated Volterra integro-differential equations. The non-linear models due to Rivlin, Green, Pipkin, Rogers and Lockett are too complicated to use with regard to geometries that one encounters in realistic physical problems. Recently, a rate-type model based on a multi-network approach, based on a proper thermodynamic foundation, has been developed by Rajagopal and Srinvasa [16] that describes well the response of a large class of viscoelastic bodies. However, they restrict their attention to small displacement gradients. Their approach can be generalized to take into account bodies undergoing large deformations. Here, we study the response to the constitutive relation developed in [17] that is an algebraic expression of the Cauchy stress, the left Cauchy–Green tensor and the symmetric part of the velocity gradient, and the model is not restricted to describing the response to small displacement gradients.

In a recent paper Bustamante et al. [17] developed a constitutive relation for the response of viscoelastic solid bodies wherein the stress, the Cauchy–Green tensor and the symmetric part of the velocity gradient are related implicitly and using standard representation theorems in continuum mechanics (see Spencer [18]) developed constitutive relations, which they then simplified to be amenable to use taking into consideration that the material should describe shear thinning as well as dependence of the material moduli on the mean value of the stress (mechanical pressure). They then used this model to study simple boundary value problems. The problems that they studied were restricted to homogeneous deformations of a slab, that is, deformations wherein the matrix for the deformation gradient in a Cartesian coordinate system has constant entries. However, even within the context of very simple homogeneous deformations of the slab that they considered, the equations governing the motion for the general class of models were non-linear and not amenable to an analytical solution and had to be solved numerically. In the case of some sub-classes of the models that they considered, they were able to find exact analytical solutions.

In this paper, we study a class of inhomogeneous problems within the context of the implicit models for the response of viscoelastic bodies developed by Bustamante et al. [17], namely the time-dependent deformation of an inclined viscoelastic layer due to the action of gravity, a problem that has relevance in geo-mechanics, where one could model certain geo-materials as being viscoelastic. The governing equations reduce to a system of non-linear equations, which under certain approximations can be solved analytically. We also solve the

* Corresponding author.
E-mail address: rogbusta@ing.uchile.cl (R. Bustamante).

https://doi.org/10.1016/j.ijnonlinmec.2020.103560
Received 6 March 2020; Received in revised form 17 June 2020; Accepted 17 July 2020
Available online 29 July 2020

Table 1
Material constants for the model (3).

μ_0	[Pa s]	6.9×10^7, 6.24×10^9
δ	1/[Pa]	8×10^{-9}
β	[s^2]	1, 10
n		−0.5, 0, 0.5
γ		0, 9.52, 95.2, 952, 9520, 47 600
λ	[Pa]	0, 9.52, 952, 95 200, 1.05×10^5, 9.52×10^6
m		0, 1, 5, 10

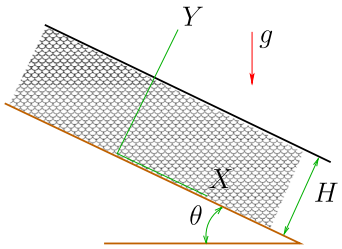

Fig. 1. Inclined viscoelastic solid slab under the influence of gravity.

fully non-linear problem, numerically. Experiments corresponding to the boundary value problem studied here are not available and hence the results of our study cannot be corroborated against experiments.

The arrangement of the paper is as follows. In Section 2 after introducing the basic kinematics relevant to the problem, we record the equation of motion, and the implicit constitutive relations that we shall use to study the boundary value problems. In Section 3 the problem of the deformation of an inclined slab under gravity is studied.

2. Basic equations

The deformation gradient, the left Cauchy–Green tensor, and the symmetric part of the velocity gradient are defined through $\mathbf{F}=\frac{\partial\chi}{\partial\mathbf{X}}$, $\mathbf{B}=\mathbf{F}\mathbf{F}^{\mathrm{T}}$, $\mathbf{D}=\frac{1}{2}\left[\frac{\partial\dot{\mathbf{x}}}{\partial\mathbf{x}}+\frac{\partial\dot{\mathbf{x}}}{\partial\mathbf{x}}^{\mathrm{T}}\right]$. The Cauchy stress tensor denoted by $\mathbf{T}$ satisfies the balance of linear momentum

$$\rho\ddot{\mathbf{x}}=\operatorname{div}\mathbf{T}+\rho\mathbf{b}, \tag{1}$$

where ρ is the density of the body and $\mathbf{b}$ represents the body forces in the current configuration, and where we use the notation $[\,\dot{}\,]$ for the material time derivative.

Here, once again we study a special sub-class of the implicit model for a visco-elastic body whose constitutive relation takes the form: $\mathfrak{F}(\mathbf{T},\mathbf{B},\mathbf{D})=\mathbf{0}$ (see Eq. (4) of [17])

$$\mathbf{T}+\varphi\mathbf{I}-\lambda\mathbf{B}-\mu\mathbf{D}=\mathbf{0}, \tag{2}$$

where λ is a constant and we assume that

$$\mu=\mu(I_1,I_2)=\mu_0e^{\delta I_1}[1+\beta I_2]^n,\quad \varphi=\varphi(I_1,\det\mathbf{F})=[\gamma I_1+\lambda][\det\mathbf{F}]^m, \tag{3}$$

where μ_0, δ, β, γ, n and m are constants and

$$I_1=\operatorname{tr}\mathbf{T},\quad I_2=\frac{1}{2}\operatorname{tr}(\mathbf{D}^2). \tag{4}$$

In Table 1 we present the values of the different constants to be used in the following sections, the same values were used in [17].

3. The response of an infinitely long viscoelastic slab under the action of gravity

In this section we study the problem of an inclined slab, as depicted in Fig. 1, due to the effect of gravity.

In the reference configuration the slab is defined by

$$-\infty\le X\le\infty,\quad 0\le Y\le H,\quad -\infty\le Z\le\infty, \tag{5}$$

We assume that the stress distribution in the slab is of the form

$$\mathbf{T}=\sum_{i=1}^{3}\sigma_i(y,t)\mathbf{e}_i\otimes\mathbf{e}_i+\tau(y,t)[\mathbf{e}_1\otimes\mathbf{e}_2+\mathbf{e}_2\otimes\mathbf{e}_1]. \tag{6}$$

We suppose that the above stress leads to a deformation field of the form

$$x=X+u(Y,t),\quad y=Y+v(Y,t),\quad z=Z. \tag{7}$$

In this case the deformation gradient, the matrices with respect to a Cartesian co-ordinate system associated with the left Cauchy–Green tensor and the symmetric part of the velocity gradient $\mathbf{D}$ take the form:

$$\mathsf{F}=\begin{bmatrix}1&u_Y&0\\0&1+v_Y&0\\0&0&1\end{bmatrix},\quad \mathsf{B}=\begin{bmatrix}1+u_Y^2&u_Y\{1+v_Y\}&0\\u_Y\{1+v_Y\}&\{1+v_Y\}^2&0\\0&0&1\end{bmatrix},$$
$$\mathsf{D}=\begin{bmatrix}0&\frac{1}{2}\frac{\dot{u}_Y}{\{1+v_Y\}}&0\\\frac{1}{2}\frac{\dot{u}_Y}{\{1+v_Y\}}&\frac{\dot{v}_Y}{\{1+v_Y\}}&0\\0&0&0\end{bmatrix}, \tag{8}$$

where we have used the notation $u_Y=\frac{\partial u}{\partial Y}$, $v_Y=\frac{\partial v}{\partial Y}$, and we have used the relations $\frac{\partial Y}{\partial y}=\frac{1}{1+v_Y}$ and $\frac{\partial\dot{u}}{\partial y}=\frac{\dot{u}_Y}{1+v_Y}$ and $\frac{\partial\dot{v}}{\partial y}=\frac{\dot{v}_Y}{1+v_Y}$.

It follows from (6) and $\mathbf{b}=g\sin\theta\mathbf{e}_1-g\cos\theta\mathbf{e}_2$ that the equations of motion take the form

$$\rho\ddot{u}=\frac{\partial\tau}{\partial y}+\rho g\sin\theta,\quad \rho\ddot{v}=\frac{\partial\sigma_2}{\partial y}-\rho g\cos\theta, \tag{9}$$

which taking into account the fact that $\frac{\partial Y}{\partial y}=\frac{1}{1+v_Y}$ become

$$\frac{\partial\tau}{\partial Y}+\rho[g\sin\theta-\ddot{u}]\left[1+\frac{\partial v}{\partial Y}\right]=0,\quad \frac{\partial\sigma_2}{\partial Y}-\rho[g\cos\theta+\ddot{v}]\left[1+\frac{\partial v}{\partial Y}\right]=0, \tag{10}$$

and since ρ_r, the density of the body in the reference configuration, is given through $\rho_r=\det\mathbf{F}\rho$ we have that $\rho_r=\rho\left[1+\frac{\partial v}{\partial Y}\right]$ and (10) becomes

$$\frac{\partial\tau}{\partial Y}+\rho_r[g\sin\theta-\ddot{u}]=0,\quad \frac{\partial\sigma_2}{\partial Y}-\rho_r[g\cos\theta+\ddot{v}]=0. \tag{11}$$

Moreover

$$I_1=\sigma_1+\sigma_2+\sigma_3,\quad \det\mathbf{F}=1+v_Y \tag{12}$$

and

$$I_2=\frac{\dot{u}_Y^2+2\dot{v}_Y^2}{4[1+v_Y]^2} \tag{13}$$

Using (6), (8) in (2) we obtain that

$$\sigma_1+\varphi-\lambda[1+u_Y^2]=0, \tag{14}$$

$$\sigma_2+\varphi-\lambda[1+v_Y]^2-\mu\frac{\dot{v}_Y}{[1+u_Y]}=0, \tag{15}$$

$$\sigma_3+\varphi-\lambda=0, \tag{16}$$

$$\tau-\lambda u_Y[1+v_Y]-\frac{\mu}{2}\frac{\dot{u}_Y}{[1+v_Y]}=0, \tag{17}$$

and the expressions for $\mu(I_1,I_2)$ and $\varphi(I_1,\det\mathbf{F})$ are given in (3).

The six equations (11), (14)–(17) must be solved to find $u(Y,t)$, $v(Y,t)$, $\sigma_1(Y,t)$, $\sigma_2(Y,t)$, $\sigma_3(Y,t)$ and $\tau(Y,t)$.

Regarding the boundary conditions we have

$$v(0,t)=0,\quad \sigma_2(H,t)=\hat{\sigma}_2(t),\quad \tau(H,t)=\hat{\tau}(t), \tag{18}$$

where $\hat{\sigma}_2(t)$ and $\hat{\tau}(t)$ are the external loads applied on the surface of the slab. The special case where the surface $Y=H$ is free of external loads corresponds to $\hat{\sigma}_2(t)=0$ and $\hat{\tau}(t)=0$. If we assume that at $Y=0$ the surface of the slab does not slip, then we have the additional condition

$$u(0,t)=0. \tag{19}$$

With regard to the initial conditions, we assume that

$$u(Y,0)=0,\quad \dot{u}(Y,0)=0,\quad v(Y,0)=0,\quad \dot{v}(Y,0)=0. \tag{20}$$

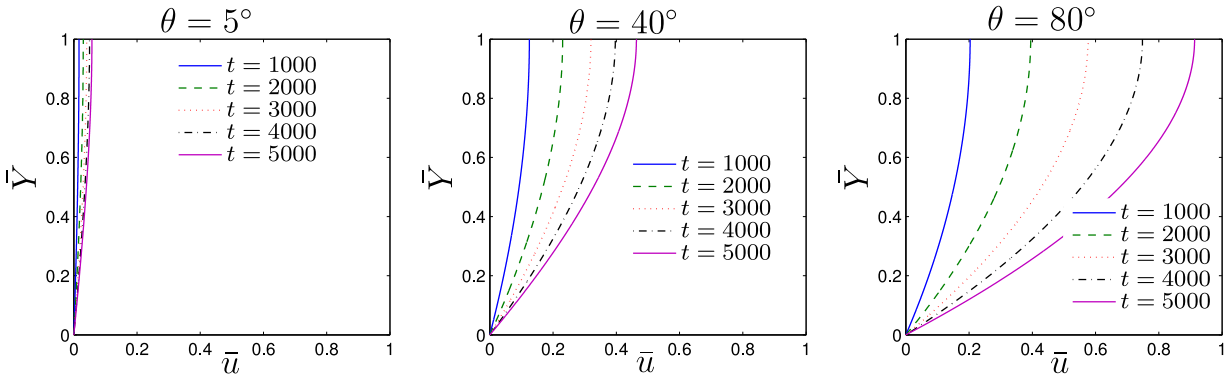

Fig. 2. The non-dimensional component $\bar{u}$ of the displacement, for different inclination angles for the slab. The times t are in seconds.

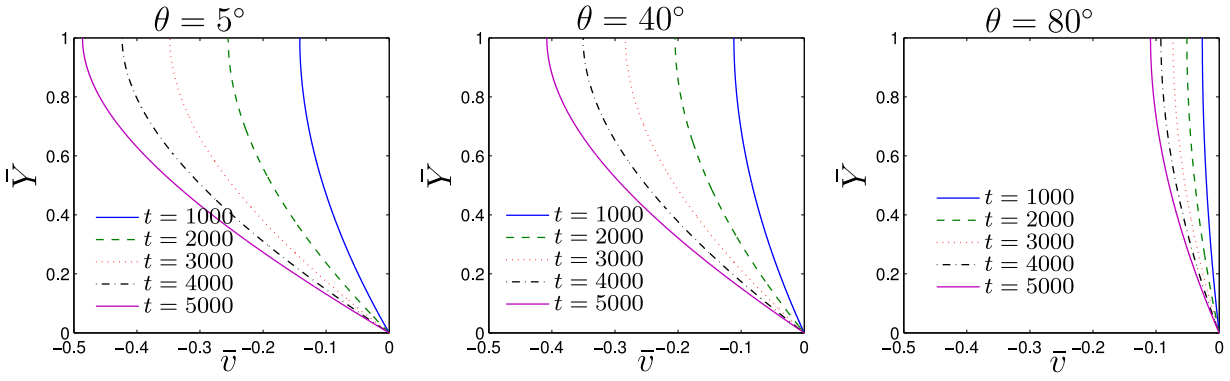

Fig. 3. The non-dimensional component $\bar{v}$ of the displacement, for different inclination angles θ for the slab. The times are in seconds.

3.1. An analytical solution for the case of small displacement gradient and $|\ddot{u}| \ll g\sin\theta$ and $|\ddot{v}| \ll g\cos\theta$

Let us study the case when we assume that $\left|\frac{\partial u}{\partial Y}\right| \sim O(\tilde{\delta})$ and $\left|\frac{\partial v}{\partial Y}\right| \sim O(\tilde{\delta})$, where $\tilde{\delta} \ll 1$ and $t > 0$. In this case (10) becomes[1] (approximately)

$$\frac{\partial \tau}{\partial y} + \rho(g\sin\theta - \ddot{u}) = 0, \quad \frac{\partial \sigma_2}{\partial y} - \rho(g\cos\theta + \ddot{v}) = 0, \tag{21}$$

whereas (14)–(16) become

$$\sigma_1 + \varphi - \lambda = 0, \tag{22}$$
$$\sigma_2 + \varphi - \lambda[1 + 2v_y] - \mu\dot{v}_y = 0, \tag{23}$$
$$\sigma_3 + \varphi - \lambda = 0, \tag{24}$$
$$\tau - \lambda u_y - \frac{\mu}{2}\dot{u}_y = 0, \tag{25}$$

where because $\left|\frac{\partial u}{\partial Y}\right| \sim O(\tilde{\delta})$ and $\left|\frac{\partial v}{\partial Y}\right| \sim O(\tilde{\delta})$ we have that $u_Y \approx \frac{\partial u}{\partial y} = u_y$ and $v_Y \approx \frac{\partial v}{\partial y} = v_y$, and where $\dot{u}_y = \frac{\partial^2 u}{\partial y \partial t}$, $\dot{v}_y = \frac{\partial^2 v}{\partial y \partial t}$. From (22) and (24) we have that $\sigma_3 = \sigma_1$.

If $|\ddot{u}| \ll g\sin\theta$ and $|\ddot{v}| \ll g\cos\theta$ in (21) after integrating we obtain

$$\tau(y,t) = -\rho g y\sin\theta + \tau_o(t), \quad \sigma_2(y,t) = \rho g y\cos\theta + \sigma_{2_o}(t). \tag{26}$$

From the boundary conditions $(18)_{2,3}$ we obtain $\tau_o(t) = \hat{\tau}(t) + \rho g\sin\theta H$ and $\sigma_{2_o}(t) = \hat{\sigma}_2(t) - \rho g\cos\theta H$, and so from (26) we have

$$\tau(y,t) = \rho g\sin\theta(H - y) + \hat{\tau}(t), \quad \sigma_2(y,t) = \rho g\cos\theta(y - H) + \hat{\sigma}_2(t). \tag{27}$$

[1] In this case there is no need to distinguish between the reference and current configurations, therefore we use $\frac{\partial}{\partial y}$ instead $\frac{\partial}{\partial Y}$. Also if $\left|\frac{\partial u}{\partial Y}\right| \sim O(\tilde{\delta})$ and $\left|\frac{\partial v}{\partial Y}\right| \sim O(\tilde{\delta})$, where $\tilde{\delta} \ll 1$ then $\rho_r \approx \rho$.

Since $\left|\frac{\partial u}{\partial Y}\right| \sim O(\tilde{\delta})$ and $\left|\frac{\partial v}{\partial Y}\right| \sim O(\tilde{\delta})$, and assuming further that[2] $|\dot{u}_Y| \sim O(\tilde{\delta})$, $|\dot{v}_Y| \sim O(\tilde{\delta})$, where $\tilde{\delta} \ll 1$ and $t > 0$, one can obtain the following approximation:

$$\varphi = [\gamma I_1 + \lambda][1 + v_y]^m \approx [\gamma I_1 + \lambda][1 + mv_y], \tag{28}$$
$$I_2 \approx 0 \quad \Rightarrow \quad \mu = \mu_0 e^{\delta I_1}[1 + \beta I_2]^m \approx \mu_0 e^{\delta I_1}, \tag{29}$$
$$[\det \mathbf{F}]^m \approx [1 + v_y]^m \approx 1 + mv_y. \tag{30}$$

Therefore, from (22)–(25) since (22) and (24) are the same, we obtain

$$\sigma_1 + [\gamma I_1 + \lambda][1 + mv_y] - \lambda = 0, \tag{31}$$
$$\sigma_2 + [\gamma I_1 + \lambda][1 + mv_y] - \lambda[1 + 2v_y] - \mu_0 e^{\delta I_1}\dot{v}_y = 0, \tag{32}$$
$$\tau - \lambda u_y - \frac{\mu_0}{2}e^{\delta I_1}\dot{u}_y = 0, \tag{33}$$

where $I_1 = 2\sigma_1 + \sigma_2$. From (31) we have $\sigma_1 = \frac{\lambda - [\gamma\sigma_2 + \lambda][1 + mv_y]}{1 + 2\gamma + 2\gamma mv_y}$ and since $[1 + 2\gamma + 2\gamma mv_y]^{-1} \approx \frac{1}{[1+2\gamma]}\left\{1 - \frac{2\gamma m}{[1+2\gamma]}v_y\right\}$ we obtain

$$\sigma_1 \approx -f_1(y,t) - f_2(y,t)v_y, \tag{34}$$

where we have defined

$$f_1(y,t) = \frac{\gamma\sigma_2}{[1 + 2\gamma]}, \quad f_2(y,t) = m\frac{[\lambda + 2\gamma\lambda + \gamma\sigma_2]}{[1 + 2\gamma]^2}. \tag{35}$$

[2] In order to be able say that $|\dot{u}_Y| \sim O(\tilde{\delta})$, $|\dot{v}_Y| \sim O(\tilde{\delta})$, where $\tilde{\delta} \ll 1$, we need to compare such quantities with something else. Note that the derivatives $\dot{u}_Y$ and $\dot{v}_Y$ have units of 1/time. Let us define t^* as some characteristic value for time, for example, the time t_o that appeared in Section 3.1 of [17]. Then, defining the dimensionless time $\bar{t} = t/t^*$ we have $\partial^2 u/\partial t\partial Y = 1/t^*\partial^2 u/\partial\bar{t}\partial Y$ and $\partial^2 v/\partial t\partial Y = 1/t^*\partial^2 v/\partial\bar{t}\partial Y$. The quantities $\partial^2 u/\partial\bar{t}\partial Y$ and $\partial^2 v/\partial\bar{t}\partial Y$ are dimensionless, and now we can assume the special cases $\left|\partial^2 u/\partial\bar{t}\partial Y\right| \sim O(\tilde{\delta})$, $\left|\partial^2 v/\partial\bar{t}\partial Y\right| \sim O(\tilde{\delta})$ $\tilde{\delta} \ll 1$.

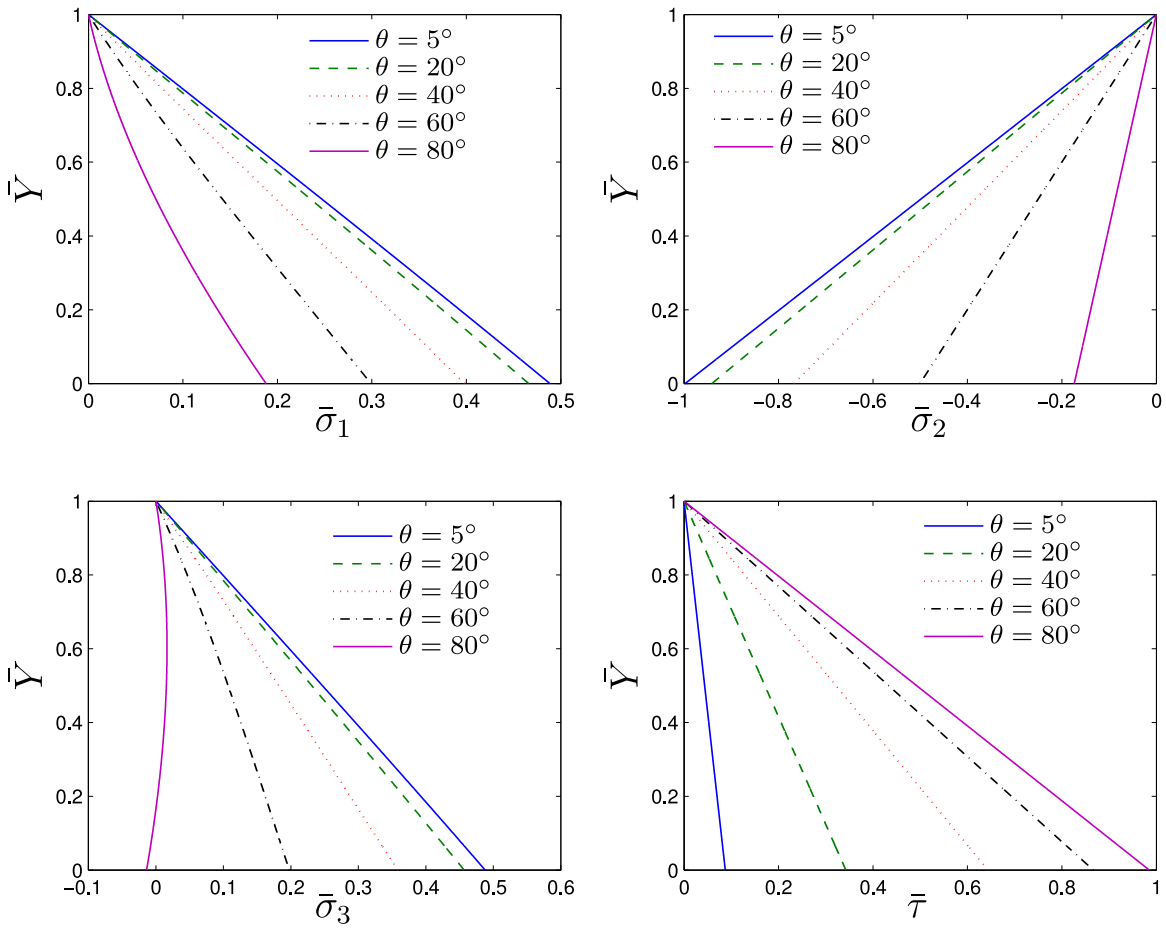

Fig. 4. Variation of $\bar{\sigma}_i$, $i = 1, 2, 3$ and $\bar{\tau}$ with respect to Y for different inclination angles θ for the slab. The results are provided for time $t = 5000$ s.

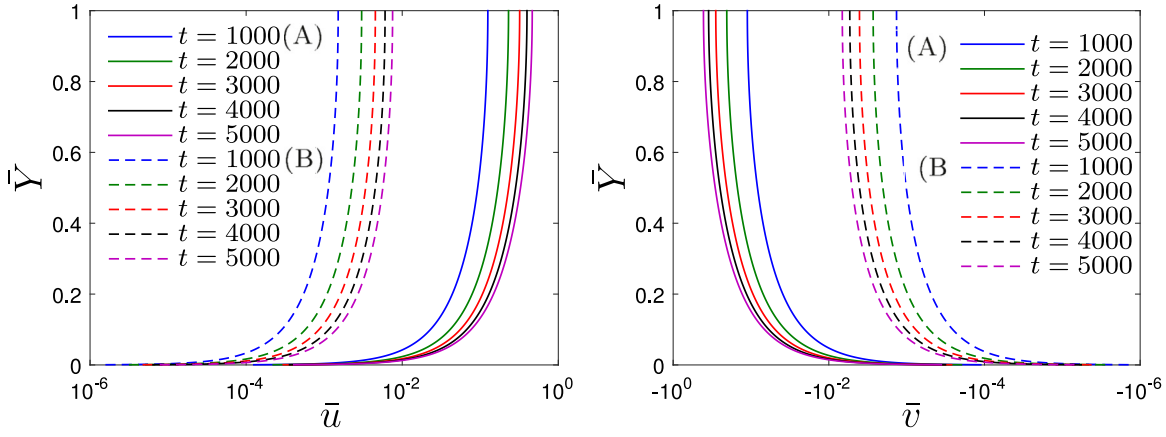

Fig. 5. Variation of $\bar{u}$ and $\bar{v}$ with respect to Y for two values for the constant μ_0. (A) $\mu_0 = 6.9 \times 10^7$, (B) $\mu_0 = 6.24 \times 10^9$.

On the other hand from (34) we have $e^{\delta I_1} = e^{\delta[2\sigma_1+\sigma_2]} \approx e^{\delta[-2f_1-2f_2 v_y+\sigma_2]}$ and considering that $|v_y| \sim O(\tilde{\delta})$ we obtain

$$e^{\delta I_1} \approx [1 - 2\delta f_2 v_y] e^{\delta[\sigma_2 - 2f_1]}. \tag{36}$$

Using (34) and (36) in (32) and (33) and recognizing that $|v_y| \sim O(\tilde{\delta})$, $|u_y| \sim O(\tilde{\delta})$ and $|\dot{v}_y| \sim O(\tilde{\delta})$, $|\dot{u}_y| \sim O(\tilde{\delta})$ we finally obtain the approximate equations

$$g_1 + g_2 v_y - g_3 \dot{v}_y = 0, \tag{37}$$

$$\tau - \lambda u_y - \frac{g_3}{2} \dot{u}_y = 0, \tag{38}$$

where we have defined

$$g_1 = g_1(y,t) = \sigma_2[1+\gamma] - 2\gamma f_1, \tag{39}$$

$$g_2 = g_2(y,t) = [\gamma\sigma_2 - 2\gamma f_1 + \lambda]m - 2[\gamma f_2 + \lambda], \tag{40}$$

$$g_3 = g_3(y,t) = \mu_0 e^{\delta[\sigma_2 - 2f_1]}. \tag{41}$$

Eqs. (37) and (38) are two linear partial differential equations that must be solved to obtain $u(y,t)$ and $v(y,t)$, where the expressions for σ_2 and τ are given through (27). As a consequence of the boundary and initial conditions $v(0,t) = 0$, $v(y,0) = 0$, $u(0,t) = 0$ and $u(y,0) = 0$, the solutions

to (37) and (38) are

$$v(y,t) = \int_0^y \left\{ \exp\left(\int_0^t \frac{g_2(\eta,\zeta)}{g_3(\eta,\zeta)}\,\mathrm{d}\zeta \right) \left[\int_0^t \frac{1}{g_3(\eta,\xi)} \times \exp\left(-\int_0^\xi \frac{g_2(\eta,\zeta)}{g_3(\eta,\zeta)}\,\mathrm{d}\zeta \right) g_1(\eta,\xi)\,\mathrm{d}\xi \right] \right\} \mathrm{d}\eta, \tag{42}$$

$$u(y,t) = \int_0^y \left\{ \exp\left(\int_0^t \frac{-2\lambda}{g_3(\eta,\zeta)}\,\mathrm{d}\zeta \right) \left[\int_0^t \frac{2}{g_3(\eta,\xi)} \times \exp\left(\int_0^\xi \frac{2\lambda}{g_3(\eta,\zeta)}\,\mathrm{d}\zeta \right) \tau(\eta,\xi)\,\mathrm{d}\xi \right] \right\} \mathrm{d}\eta. \tag{43}$$

Let us consider the special case when in (27) we assume that $\hat{\tau}(t) = \hat{\tau}_o$ and $\hat{\sigma}_2(t) = \sigma_{2_o}$ do not depend on time, therefore $\tau = \tau(y)$ and $\sigma_2 = \sigma_2(y)$ and we have $g_i = g_i(y)$, $i = 1,2,3$. In this case, from (42) and (43) we obtain

$$v(y,t) = \int_0^y \left\{ \frac{1}{g_2(\eta)} \left[\exp\left(\frac{g_2(\eta)t}{g_3(\eta)} \right) - 1 \right] g_1(\eta) \right\} \mathrm{d}\eta, \tag{44}$$

$$u(y,t) = \int_0^y \left\{ \frac{1}{\lambda} \left[1 - \exp\left(\frac{-2\lambda t}{g_3(\eta)} \right) \right] \tau(\eta) \right\} \mathrm{d}\eta. \tag{45}$$

3.1.1. A qualitative analysis of the solutions for $t \gg 1$

Taking $U = u_y$ and $V = v_y$ from (37) and (38) we obtain

$$\frac{\partial U}{\partial t} = \frac{2}{g_3}[\tau - \lambda U], \quad \frac{\partial V}{\partial t} = \frac{1}{g_3}[g_1 + g_2 V]. \tag{46}$$

Assuming $\hat{\sigma}_2(t) = \sigma_{2_o}$ and $\hat{\tau}(t) = \tau_o$, the functions g_1, g_2 and g_3 only depend on y. For each y fixed $(46)_1$ is a linear system of ordinary differential equations. The steady-state solutions are $U_s = \tau/\lambda$, $V_s = -g_1/g_2$, then for $t \gg 1$ we have

$$U \approx \frac{\tau}{\lambda}, \quad V \approx -\frac{g_1}{g_2}, \tag{47}$$

then for u and v we obtain

$$\frac{\partial u}{\partial y} = \frac{-\rho g \sin\theta y + \tau_o}{\lambda}, \quad \frac{\partial v}{\partial y} = -\frac{\{[1+\gamma]\sigma_2 - 2\gamma f_1\}}{\{[\gamma\sigma_2 - 2\gamma f_1 + \lambda]m - [2\gamma f_2 + \lambda]\}}. \tag{48}$$

Defining $c_1 = \gamma m\left\{1 - \frac{\gamma}{[1+2\gamma]} - \frac{2\gamma}{[1+\gamma]^2}\right\}$, $c_2 = [m-2]\lambda - \frac{2\gamma m\lambda}{[1+2\gamma]}$ and $c_3 = \frac{1+3\gamma}{1+2\gamma}$ we obtain

$$u(y,t) = -\frac{\rho g \sin\theta}{2\lambda} y^2 + \frac{\tau_o}{\lambda} y, \tag{49}$$

$$v(y,t) = \frac{c_3}{c_1} y - \frac{c_2 c_3}{c_1^2 \rho g \cos\theta} \ln\left(\frac{c_1 \rho g \cos\theta y + c_1 \sigma_{2_o} + c_2}{c_1 \sigma_{2_o} + c_2} \right). \tag{50}$$

3.2. The fully nonlinear problem

In this section we solve the original equations (11) and (14)–(17) numerically. Eq. (11) was

$$\frac{\partial \tau}{\partial Y} + \rho_r[g\sin\theta - \ddot{u}] = 0, \quad \frac{\partial \sigma_2}{\partial Y} - \rho_r[g\cos\theta + \ddot{v}] = 0. \tag{51}$$

Let us recall (14)–(17)

$$\sigma_1 + \varphi(I_1, \det\mathbf{F}) - \lambda[1 + u_Y^2] = 0, \tag{52}$$

$$\mathcal{G} = \sigma_2 + \varphi(I_1, \det\mathbf{F}) - \lambda[1 + v_Y^2] - \mu(I_1, I_2)\frac{\dot{v}_Y}{[1+u_Y]} = 0, \tag{53}$$

$$\sigma_3 + \varphi(I_1, \det\mathbf{F}) - \lambda = 0, \tag{54}$$

$$\tau - \lambda u_Y[1 + v_Y] - \mu(I_1, I_2)\frac{\dot{u}_Y}{2[1+v_Y]} = 0, \tag{55}$$

where $I_1 = \sigma_1 + \sigma_2 + \sigma_3$, $I_2 = \frac{\dot{u}_Y^2 + 2\dot{v}_Y^2}{4[1+v_Y]^2}$ and $\det\mathbf{F} = 1 + v_Y$. We recall that the boundary and initial conditions are $v(0,t) = 0$, $v(Y,0) = 0$, $\dot{v}(Y,0) = 0$, $u(0,t) = 0$, $u(Y,0) = 0$, $\dot{u}(Y,0) = 0$, $\sigma_2(H,t) = \hat{\sigma}_2(t)$ and $\tau(H,t) = \hat{\tau}(t)$.

From (55) we obtain

$$\tau = \lambda u_Y[1 + v_Y] + \mu(I_1, I_2)\frac{\dot{u}_Y}{2[1+v_Y]}. \tag{56}$$

On the other hand if we use the expression for φ given in (3) from (54) we can obtain σ_3 as

$$\sigma_3 = \frac{\lambda - \{\gamma[\sigma_1 + \sigma_2] + \lambda\}[\det\mathbf{F}]^m}{1 + \gamma[\det\mathbf{F}]^m}, \tag{57}$$

and since $\gamma > 0$ and $\det\mathbf{F} > 0$ the above expression is always valid. Using the above expression in (52) we can obtain σ_1 as

$$\sigma_1 = \frac{\{1 + u_Y^2 + [\gamma u_Y^2 - 1][\det\mathbf{F}]^m\}\lambda - \gamma\sigma_2[\det\mathbf{F}]^m}{1 + 2\gamma[\det\mathbf{F}]^m}, \tag{58}$$

as a result from (57) we have

$$\sigma_3 = \frac{\lambda - [\lambda + \gamma\lambda u_Y^2 + \gamma\sigma_2][\det\mathbf{F}]^m}{1 + 2\gamma[\det\mathbf{F}]^m}. \tag{59}$$

In view of the above results, from (53) we have one equation for σ_2. Let us assume that the basic variables for the problem are $u(Y,t)$ and $v(Y,t)$. From (53) we have an expression of the form

$$\mathcal{G}(\sigma_2, u_Y, \dot{u}_Y, v_Y, \dot{v}_Y) = 0,$$

We can numerically find σ_2 in terms of u_Y, $\dot{u}_Y$, v_Y and $\dot{v}_Y$ from the above equation using Newton's method, therefore, in particular we will have

$$\tau = \tau(u_Y, \dot{u}_Y, v_Y, \dot{v}_Y), \quad \sigma_2 = \sigma_2(u_Y, \dot{u}_Y, v_Y, \dot{v}_Y), \tag{60}$$

which can be replaced in (51). Using the above assumptions, the Eqs. (51) are solved employing the finite element method using the programme Comsol 3.4 [19].

The following figures portray the components of the displacement field, and the components of the stress tensor, as a result of solving (51) for the different cases for the constants that appear in Table 1, and also for different values for the angle θ depicted in Fig. 1. In all these cases we assumed that $\rho_r = 1500\ \mathrm{kg/m^3}$. A study of the influence of the mesh on the results was performed, and we found that for the mesh used in this problem with 3842 degrees of freedom, there is no influence of the mesh on the final results. We have used the following non-dimensionalization:

$$\bar{Y} = \frac{Y}{H}, \quad \bar{u} = \frac{u}{H}, \quad \bar{v} = \frac{v}{H} \quad \bar{\sigma}_i = \frac{\sigma_i}{\rho_r g H}, \quad i = 1,2,3, \quad \bar{\tau} = \frac{\tau}{\rho_r g H}, \tag{61}$$

as well as $H = 1$ m and $g = 9.8\ \mathrm{m/s^2}$.

In Fig. 2 we have results for $\bar{u}$ for different angles of inclination θ of the slab (see Fig. 1), at different times. As expected, larger displacement fields are obtained for larger values for θ. For the results presented in this plot as well as in the following figures, it is necessary to point out that in order to obtain relatively large displacement fields and deformations, relatively large time intervals have to elapse.

In Fig. 3 we present similar results in this case for $\bar{v}$. As is to be expected, the displacement is negative, and that magnitude of that component decreases with increasing inclination angles θ.

In Fig. 4 results are presented for the non-dimensional stresses $\bar{\sigma}_i$, $i = 1,2,3$ and $\bar{\tau}$ for different inclination angles θ for the slab. The results are only presented for the case $t = 5000$ s, this is because we observed small differences for the components of the stress over time. This is due to the effect of acceleration being very small in comparison with the effect of gravity. This would suggest that the following approximation would be valid (see (27))

$$\tau(Y,t) = \rho_r g \sin\theta[H - Y] + \hat{\tau}(t), \quad \sigma_2 = \rho_r g \cos\theta[Y - H] + \hat{\sigma}_2(t), \tag{62}$$

which would be the approximate solutions of Eqs. (51), where we see that σ_2 and τ are linear functions in Y, which is what is observed in the results presented in Fig. 4. We choose to solve (51) directly since that is amenable from the numerical point of view using the finite element method. With regard to the solutions depicted in Figs. 2–4 we assumed that $\mu_0 = 6.9 \times 10^7$, $\beta = 1$, $\gamma = 95.2381$, $\lambda = 952.381$, $n = 0$ and $m = 1$.

In Fig. 5 we have results for the displacements $\bar{u}$ and $\bar{v}$ for the two values of μ_0 presented in Table 1 (see (3)), at different times. From

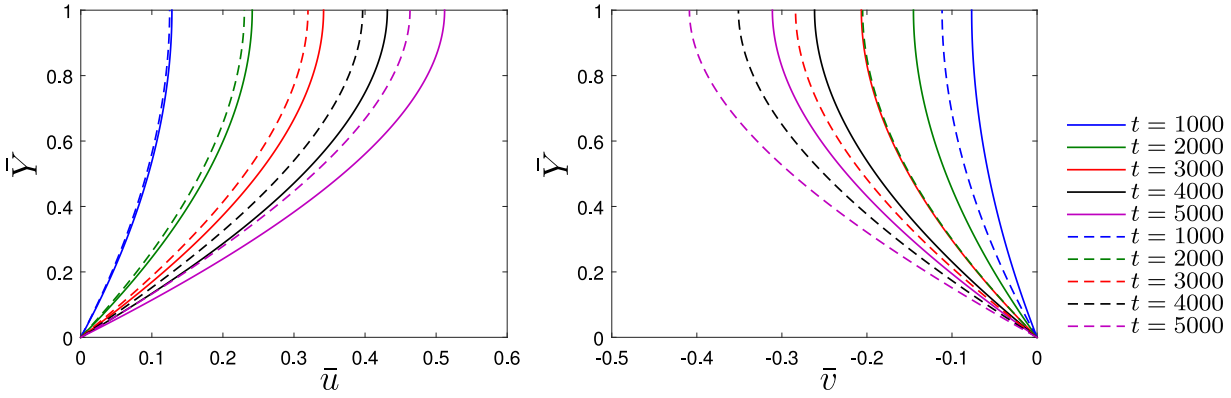

Fig. 6. Variation of $\bar{u}$ and $\bar{v}$ with respect to Y. Continuous lines $\gamma = 0$. Dashed lines $\gamma = 4.76 \times 10^4$.

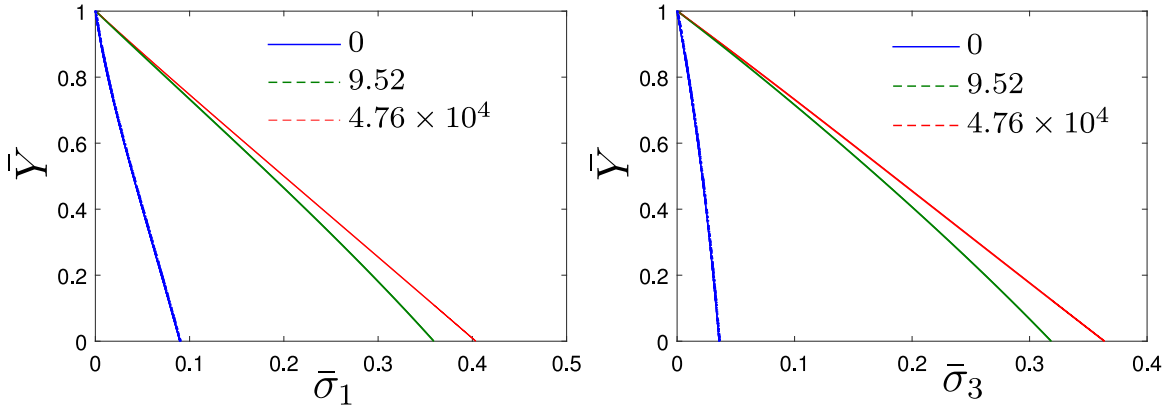

Fig. 7. Variation of $\bar{\sigma}_1$ and $\bar{\sigma}_3$ with respect to Y for the different values for γ presented in Table 1, for the instant $t = 5000$ s.

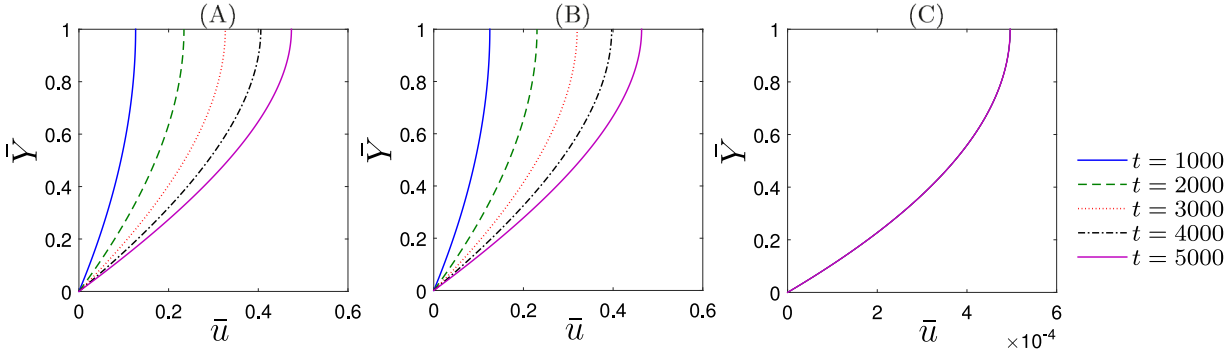

Fig. 8. Variation of $\bar{u}$ with respect to Y for different values of λ. (A) $\lambda = 0$, (B) $\lambda = 952$, (C) $\lambda = 9.52 \times 10^6$.

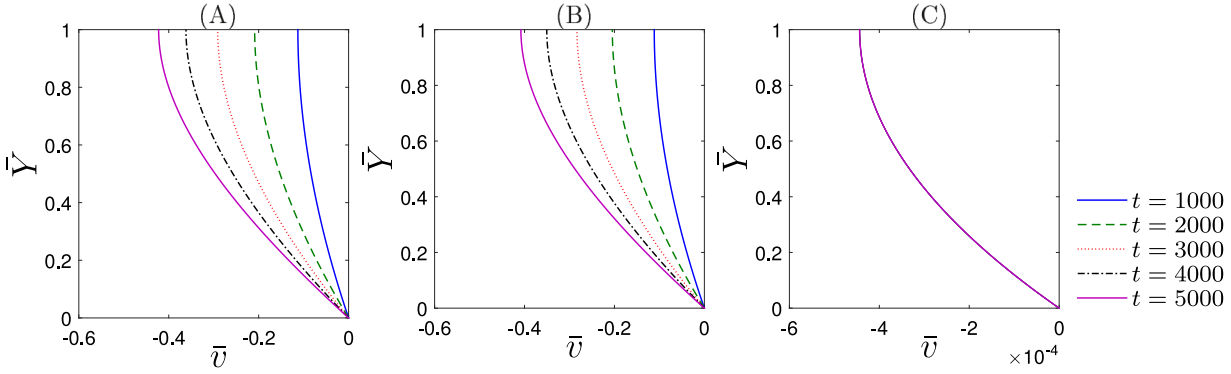

Fig. 9. Variation of $\bar{v}$ with respect to Y for different values of λ. (A) $\lambda = 0$, (B) $\lambda = 952$, (C) $\lambda = 9.52 \times 10^6$.

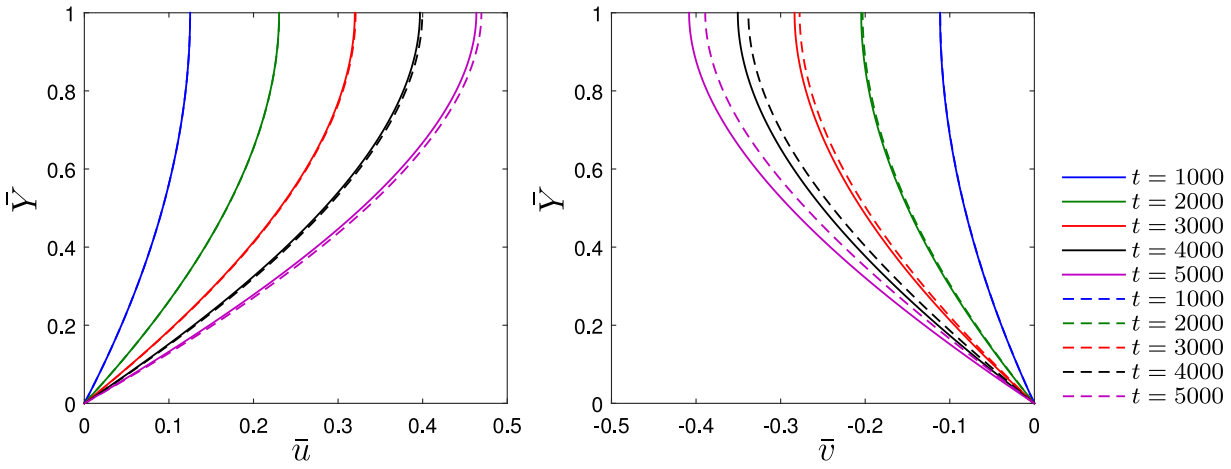

Fig. 10. Variation of $\bar{u}$ and $\bar{v}$ with respect to Y for two values for the constant m. Continuous lines represent case $m = 0$, dashed lines represent case $m = 10$.

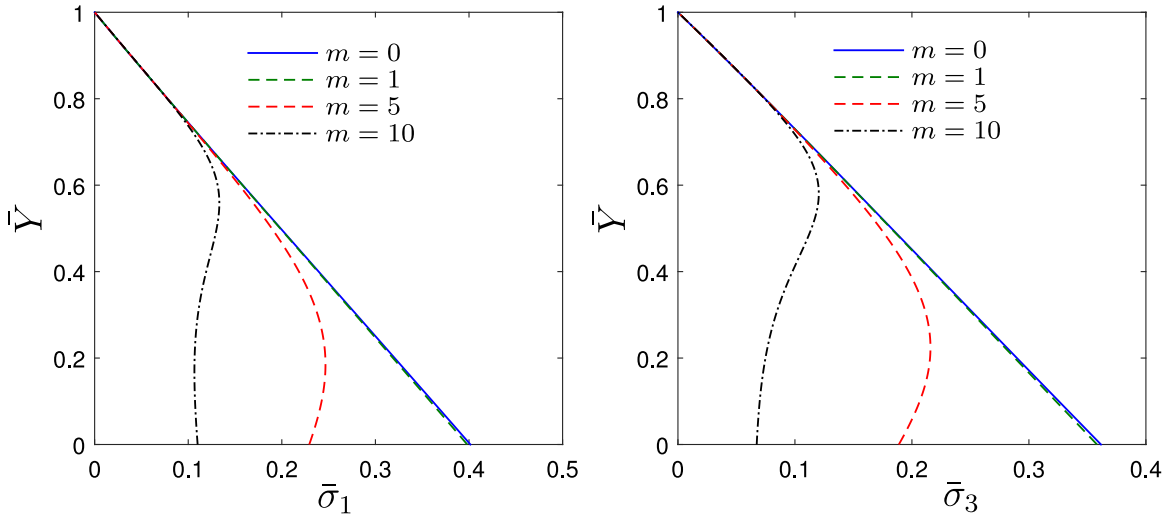

Fig. 11. Variation of $\bar{\sigma}_1$ and $\bar{\sigma}_3$ with respect to Y for two values for the constant m and for $t = 5000$ s.

these plots one can infer that in the case of $\bar{u}$, larger deformations are observed if μ_o is smaller, i.e., when the viscosity μ is smaller (see (3)), which is what one would expect. Now, with regard to the influence of μ_0 on the components of the stress, it is observed that they change very little at different times, and that the distributions for $\bar{\sigma}_2$ and $\bar{\tau}$ are almost the same for the two different values for μ_0 (see the comments regarding (62)). Only $\bar{\sigma}_1$ and $\bar{\sigma}_3$ are affected for the different values of μ_0, in particular in the case when $\bar{\sigma}_1$ is greater, and $\bar{\tau}$ is smaller. For the sake of brevity those results are not presented in this paper. With regard to the results presented in Fig. 5 we assumed that $\theta = 40°$, $\beta = 1$, $\gamma = 95.2381$, $\lambda = 952.381$, $n = 0$ and $m = 1$.

In the case of the two different values for β presented in Table 1, from (3) we can see that the effect of changing the constants would be more important if I_2 is larger, and from (13) that invariant depends on the squares of $\dot{u}_Y$ and $\dot{v}_Y$. In the present problem, the body deforms due to the effect of gravity, and from the numerical results it is observed that $\dot{u}_Y$ and $\dot{v}_Y$ are small, therefore, the effect of changing β on $\bar{u}$, $\bar{v}$, $\bar{\sigma}_i$, $i = 1, 2, 3$ and $\bar{\tau}$ is negligible, and in view of this we do not present plots for these cases. For the same reasons, there is not much difference in the behaviour of the displacement and the stress as I_2 is small. We do not show results for the different values of n in Table 1 as well.

In Fig. 6 results are presented for $\bar{u}$ and $\bar{v}$ for two different values for γ (see Table 1 and (3)), namely $\gamma = 0$ and $\gamma = 4.76\times10^4$, and for different times. We found that over a wide range of values for γ the values for u and v are nearly the same and hence we only show representative figures. From Fig. 6, in the case of $\bar{u}$ we can see that for a larger γ the body becomes softer, i.e., it deforms more, the same happens for the magnitude of $\bar{v}$.

In Fig. 7 we have results for $\bar{\sigma}_1$ and $\bar{\sigma}_3$ for different values for γ presented in Table 1, for the instant $t = 5000$ s. In the case of $\bar{\sigma}_2$ and $\bar{\tau}$, such components of the stress are almost the same for the different values of γ, and plots are not presented for them. The results presented in Figs. 6 and 7 were obtained assuming that $\theta = 40°$, $\mu_0 = 6.9 \times 10^7$, $\beta = 1$, $\lambda = 952.381$, $n = 0$ and $m = 1$.

In Figs. 8 and 9 results are presented for $\bar{u}$ and $\bar{v}$ for the three different values for the constant λ from Table 1 (see (3)). In each case we display the behaviour of $\bar{u}$ and $\bar{v}$ for different times. It is interesting to notice the response of the slab when $\lambda = 9.52 \times 10^6$, there is almost no difference for the displacements $\bar{u}$, $\bar{v}$ with time, and this implies that the deformation of the slab is almost instantaneous. As λ increases (this is the constant that multiplies **B** see (2)) we expect the response of the body to be more elastic. If λ decreases we expect the viscous effects to be more significant. The results presented in these two figures were obtained assuming that $\theta = 40°$, $\mu_0 = 6.9\times10^7$, $\beta = 1$, $\gamma = 95.2381$, $n = 0$ and $m = 1$.

Finally, in Figs. 10 and 11 results are presented for different values for m given in Table 1 (see (3)). With regard to $\bar{u}$ and $\bar{v}$ we do not observe difference in the response between the results for $m = 0$, 1, and 5, which is why in Fig. 10 results are only presented for the two cases $m = 0$ and $m = 10$. For larger values of m the body becomes slightly softer. In the case of the components of the stress tensor, as in the previous cases, the components $\bar{\sigma}_2$ and τ are almost the same for the different cases for m, and results are only presented for $\bar{\sigma}_1$ and $\bar{\sigma}_3$ for $t = 5000$ s. It is interesting to note, from Fig. 11 the completely different response characteristic obtained for the two components of the stress tensor, in particular when $m = 0$, $m = 1$, and $m = 5$, $m = 10$. All these results were obtained assuming that $\theta = 40°$, $\mu_0 = 6.9 \times 10^7$, $\beta = 1$, $\gamma = 95.2381$, $\lambda = 952.381$, $n = 0$ and $m = 1$.

CRediT authorship contribution statement

R. Bustamante: Finding exact solutions, Solving the boundary value problem numerically, Proposing the constitutive model. **K.R. Rajagopal:** Proposing the constitutive model. **O. Orellana:** Solving the boundary value problem exactly for a special case. **R. Meneses:** Solving the boundary value problem exactly.

Declaration of competing interest

The authors declare that they have no known competing financial interests or personal relationships that could have appeared to influence the work reported in this paper.

Acknowledgments

R. Bustamante would like to express his gratitude for the financial support provided by FONDECYT (Chile) under grant no. 1160030. K.R. Rajagopal thanks the National Science Foundation, United States and the Office of Naval Research, United States for support of this work.

References

[1] W. Thomson, On the elasticity and viscosity of metals, Proc. R. Soc. Lond. Ser. A 14 (1865) 289–297.
[2] W. Voigt, Ueber innere reibung fester korper, insbesondere der metalle, Ann. Phys. 283 (1892) 671–693.
[3] L. Boltzmann, Zur theorie der elastichen nachwirkung, Ann. Physics 7 (1876) 624–654.
[4] C.A. Truesdell, W. Noll, in: S.S. Antmann (Ed.), The Non-Linear Field Theories of Mechanics, third ed., Springer, Berlin, Germany, 2004.
[5] F.J. Lockett, Non-Linear Viscoelastic Solids, Academic Press, London, 1972.
[6] K.R. Rajagopal, On implicit constitutive theories, Appl. Math. 48 (2003) 279–319.
[7] K.R. Rajagopal, A note on a reappraisal of the Kelvin-Voigt model, Mech. Res. Commun. 36 (2009) 232–235.
[8] M. Bulicek, J. Malek, K.R. Rajagopal, On the kelvin-voigt model and its generalizations, Evol. Equ. Control Theory 1 (2012) 17–42.
[9] R.M. Christensen, Thoery of Viscoelasticity, Academic Press, New York, 1982.
[10] A.S. Wineman, K.R. Rajagopal, Mechanical Response of Polymers: An Introduction, Cambridge University Press, 2000.
[11] Y.C. Fung, Biomechanics: Mechanical Properties of Living Tissues, Springer, New York, 1981.
[12] A.M. Muliana, K.R. Rajagopal, A.S. Wineman, A new class of quasi-linear models for describing the non-linear viscoelastic response of materials, Acta Mech. 224 (2013) 2169–2183.
[13] A.S. Wineman, Large axi-symmetric deformation of a non-linear viscoelastic membrane due to spinning, J. Appl. Mech. Trans. ASME 39 (1972) 946–952.
[14] A.S. Wineman, Large axi-symmetric deformation of a non-linear viscoelastic membrane by lateral pressure, Trans. Soc. Rheol. 20 (1976) 203–225.
[15] A.S. Wineman, Non-linear viscoelastic solids, a review, Math. Mech. Solids 14 (2009) 300–366.
[16] K.R. Rajagopal, A.R. Srinivasa, An implicit thermomechanical theory based on a Gibbs potential formulation for describing the response of thermoviscoelasti solids, Internat. J. Engrg. Sci. 20 (2013) 15–28.
[17] R. Bustamante, K.R. Rajagopal, O. Orellana, R. Meneses, Implicit constitutive relations for describing the response of visco-elastic bodies, Homog. Deform. (2020) (Accepted).
[18] A.J.M. Spencer, Theory of invariants, in: A.C. Eringen (Ed.), Continuum Physics, Vol. 1, Academic Press, New York, NY, 1971, pp. 239–353.
[19] Comsol Multiphysics, Version 3.4, Comsol Inc., Palo Alto, CA, 2007.